Bull. Astr. Soc. India (2001) **29**, 545-561

Performance of the IIA mosaic CCD camera system

B. Nagaraja Naidu[1], R. Srinivasan[1], V. Mohan[2], Ram Sagar[1,2]
[1] *Indian Institute of Astrophysics, Bangalore - 560034, India*
[2] *State Observatory, Manora Peak, Nainital - 263 129, India*

Received 13 August 2001; accepted 6 December 2001

Abstract. We evaluate performance of the 4K x 4K mosaic CCD camera system developed at the Indian Institute of Astrophysics using four Thomson CCDs in a buttable configuration. The camera system consists of a mosaic CCD dewar developed to mount the four CCDs and an electronics controller designed to control the mosaic configuration. A window based data acquisition software is used to configure the controller and acquire images from the camera. The calibration measurements indicate that all 4 CCDs have similar characteristics with a gain of about 3.9 e/ADU, rms noise of $\sim$ 19 e, full-well capacity of $\sim$ 57 000 ADU, non-linearity of $\sim$ 0.4 % and peak quantum efficiency of $\sim$ 40 % in the red region. The problem of cross-talk is faced in this multi-readout system and a solution is offered. The performance of the mosaic CCD camera has been found satisfactory at the telescope.

Key words : Mosaic CCDs – Calibration – THX7897M – Cross-talk

1. Introduction

There is a constant need for wide field imaging in optical astronomy to enable studies of star clusters, galaxies etc. While Charge Coupled Devices (CCDs) have become the choice of detectors in the field of optical astronomical imaging, due to their high quantum efficiency (Qe) and wide spectral response, there is a size limitation. The commercially available CCDs have grown from their initial size of 100 x 100 pixel^2 to the current 2048 x 4096 pixel^2 format. Aiming at large size CCD during production-run results in rather poor yield and high cost. The mosaic CCD approach can overcome this limitation, as some of the standard CCDs are now being fabricated with buttable edges which can be mounted carefully close to each other (mosaic) in various configurations to form a large CCD array.

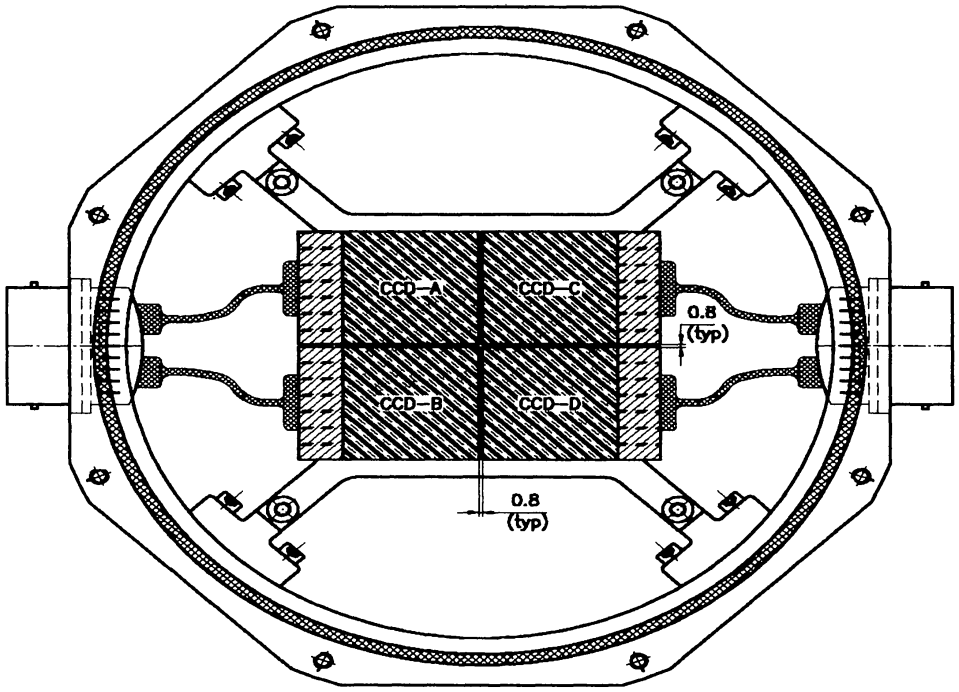

Fig.1: CAD View of the Mosaic CCD Mount

Recently Indian Institute of Astrophysics (IIA) has developed a 4K x 4K mosaic CCD camera system using the Thomson-CSF 3-edge buttable CCDs (THX7897M). In order to reduce cost, the IIA opted for a wafer-run with the Thomson-CSF to produce a 3-edge buttable 2K x 2K CCDs. The wafer-run probe tests resulted in 6 good quality CCDs. The mosaic CCD camera has been developed using 4 of these wafer-run CCDs in a 2 x 2 configuration. The complete mosaic CCDs camera system consists of a modular CCD cryostat (Naidu, Srinivasan & Nathan 2001), a versatile CCD controller (Naidu & Srinivasan 2001) and data acquisition software (Naidu, Srinivasan & Shankar 1997). Further description of the camera is given in the next section. The laboratory calibration setup, characterisation of the mosaic CCDs, the problem of cross-talk faced in this multi-readout CCD and evaluation of the performance of the system at the telescope are described in the remaining part of the paper.

2. The mosaic CCD camera system

The THX7897M CCD is a 3-edge buttable 2048 x 2048 format with 15 μm square pixels. It is a front illuminated device with UV enhancement coating and operates in multi-pinned phase mode. The device has a typical peak Qe of 35 to 40 % in the red region, 10 % in the blue and 10 % at 920 nm. It is buttable on three sides allowing for 2 x N mosaics. The device has 4 output amplifiers on each chip. An amplifier covers a section

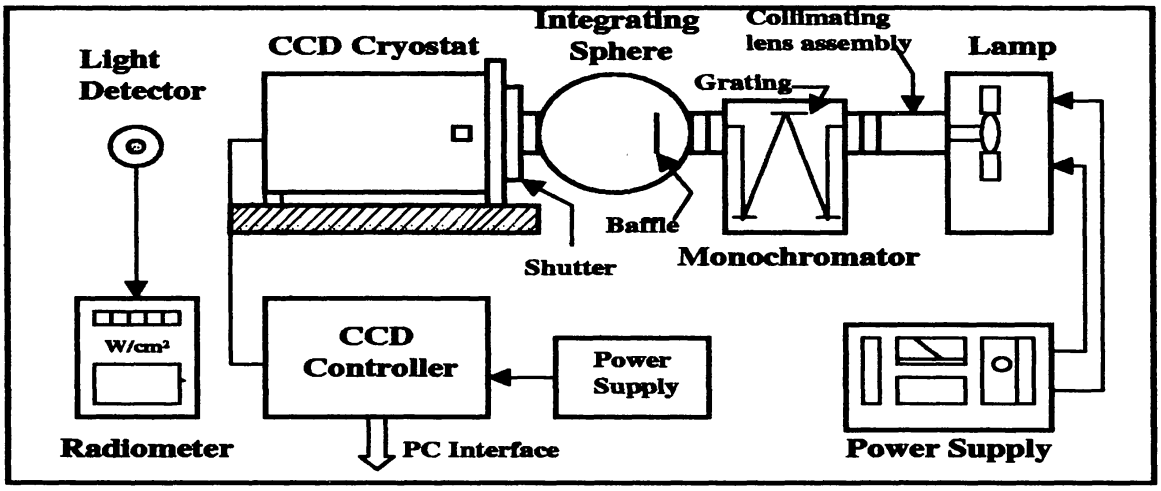

Figure 2. Laboratory setup for CCD calibration.

of 512 x 2048 pixel^2 of a chip. All the 4 amplifiers of a chip are used to read its entire area. The 16 readouts from the 4 CCDs form the inputs for the analog processing circuit in the controller. The mosaic CCD controller also generates 13 bias and 11 clock voltages for each CCD.

The individual CCDs are mounted onto a base plate inside the camera head. The CCD mount holes are drilled on the base plate at the selected positions in order to accommodate the four CCDs. The locating pins have been provided for each CCD to facilitate easy installation of the device onto the mosaic plane. Each CCD is fastened to the base plate through a set of 4 screws. The inter-gaps between the CCDs are held within 1 mm. The CCD mount is cooled down to −90°C during operation using LN2 from a container attached to the camera head. Fig. 1 presents a view of the mosaic CCD camera mount.

3. Laboratory tests

The details of the laboratory calibration setup used to characterise the CCDs and other problems of the mosaic CCD camera are described in this section.

3.1 Experimental setup

The schematic of an optical test bench setup for carrying out the laboratory tests on the mosaic CCD is shown in Fig. 2. The main components of the setup are a lamp source, a power supply, a monochromator, an integrating sphere and a light meter. A

75W Xenon lamp is mounted in a convection cooled housing with a f/1.5 collimating lens assembly. The collimated beam is 38 mm diameter and is focused on the input slit of the monochromator. The lamp is controlled by a constant current supply. The Oriel's 77200 monochromator provides 0.1 nm resolution with a 1200 lines/mm grating and narrow slit. The usable wavelength range covers from 200 nm to 1100 nm. A 20 cm diameter-integrating sphere is used to produce uniform illumination. The sphere has input and exit ports of diameters 38 mm and 50 mm respectively. The input port of the sphere is aligned to the exit port of the monochromator. A light meter IL1700 supplied by M/s International Light is used to measure the absolute light flux. This light meter uses a calibrated photo diode as detector (silicon SED033) and can measure the light intensity directly in Watt/cm^2. The detector response covers from 400 nm to 1000 nm. The integrating sphere is attached to a mounting post while the mosaic CCD dewar is mounted onto a flange. The space between the exit port of the integrating sphere and the dewar is light shielded. In order to measure the absolute light flux, the SED033 is kept at the distance of the CCD dewar.

3.2 Noise and gain characterization

The gain of a CCD system can be determined approximately if the sensitivity of the on-chip output amplifier and the signal processing gain are known. It is given as

$$\text{System Gain (electron/ADU)} = (\text{SV*A*IG*ADC}_{CONV})^{-1},$$

where SV is the output sensitivity of the CCD in μV/electron, A is the pre-amplifier gain, IG is the dual slope integration gain of the signal processing chain and ADC_{CONV} is the analog to digital converter (ADC) conversion factor in (ADU/μV). For the THX7897 CCDs typical sensitivity is 4.2 μV/electron. Hence, the calculated system gain is

$$(4.2\mu\text{V/electron} * 1.0 * 5.0 * 1\ \text{ADU}/68.67\mu\text{V})^{-1} = 3.27\ \text{electron/ADU}.$$

The gain of the camera can be determined more accurately by measuring the shot noise as a function of the input flux at high levels where the shot noise dominates the readout noise. The method is called as photon transfer technique, developed first by Janesick, Klaasen & Elliott (1987) as a tool to calibrate gain of a CCD system. The transfer curve is a plot of the variance (square of noise) versus the mean counts of an image frame after pixel to pixel non-uniformity is removed (flat-fielded) by a simple process, which is described below. The variance in the signal, σ_e^2, in electrons of such a frame is given by

$$\sigma_e^2 = (\text{Photon noise})^2 + (\text{Readout noise})^2.$$

Assuming Poisson statistics, (Photon noise)^2 is the signal in electrons which is the in-

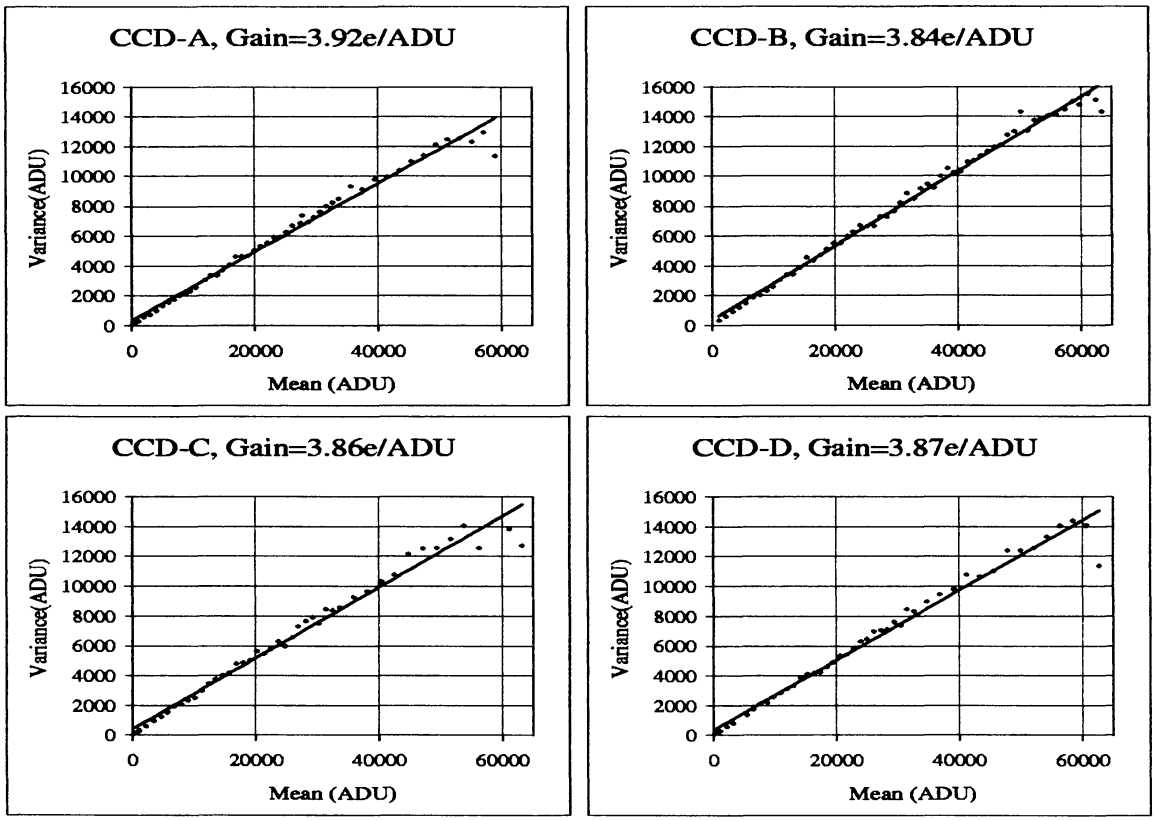

Figure 3. Photon transfer plots for individual CCDs of the IIA mosaic camera.

tensity in ADU multiplied by the gain (g) of the camera system in electron/ADU, the relation can be written as

$$(\sigma_{ADU})^2 = 1/\mathrm{g} * (\mathrm{I}_{ADU}) + (\text{Readout noise/g})^2.$$

So, the inverse of the slope of the plot of $(\sigma_{ADU})^2$ versus (I_{ADU}) is the gain in units of electron/ADU. The readout noise can be obtained by multiplying the σ_{ADU} of a bias frame (zero photon noise) with the system gain. In order to use the above relation to determine gain and readout noise, we carried out the following measurements.

The input and output slits of the monochromator were adjusted such that a count rate around 1000/sec is obtained. Several pairs of flat images with counts ranging from above the bias level to near saturation were obtained by varying exposure times. The exposure times for pair of flats are kept same. The pixel non-uniformity is removed by

Table 1. The CCD parameters derived from the calibration measurements.

Parameter	CCD-A	CCD-B	CCD-C	CCD-D
Gain (electron/ADU)	3.92	3.84	3.86	3.87
Rms-noise (electron)	19.2	19.2	18.4	18.8
Full-well (ADU)	57,000	58,000	56,200	58,000
Full-well (electron)	223,440	222,720	216,932	224,460
Non-linearity (% P-V)	0.39	0.43	0.3	0.46

subtracting the two similar flats obtained with same exposures under identical conditions. On such frames, the variance is calculated for a small region (40 x 40 pixel^2) free from pixel defects. The variance of the difference flat is divided by 2 as the noise in the difference flat is increased by $\sqrt{2}$ because of subtraction. The mean levels from the same region in both frames are computed and averaged after subtracting a mean bias level. Similarly, the variance and the mean were obtained for all pairs of the flat images. The photon transfer plots for the 4 CCDs are shown in Fig. 3. A straight line is fitted to the data points excluding saturated points. The reciprocal of the slope of the straight line gives the conversion factor of the readout chain. The gain and noise for all the 4 readouts in each CCD are thus obtained. The noise rollover is caused by saturation effects as the full-well capacity is reached and the counts do not follow Poisson statistics any more. Table 1 presents the gain, noise and full-well capacities obtained from photon transfer plots for all the 4 CCDs in the mosaic.

3.3 Quantum efficiency measurements

The Qe is a measure of the efficiency with which the incident photons are detected. For $\lambda > 300$ nm, each photon generates one electron-hole pair. The Qe as a function of the response of the device can be expressed as (Buil Christian 1991)

$$\text{Qe} = \text{Response(A/W)} * \frac{h \times c}{q \times \lambda} = \frac{N_e \times q}{P \times S} * \frac{h \times c}{q \times \lambda} = \frac{1.989 * 10^{-25} N_e}{P \times S \times \lambda},$$

where h is the Planck's constant (6.63 * 10^{-34} J.s), c is the velocity of light (3 * 10^8 m/s), q is electron's charge (1.6 * 10^{-19} Coulombs), N_e is number of collected electrons per pixel per second, P is the optical power density in Watt/cm^2, S is the area of a CCD pixel in cm^2 and λ is the wavelength in meter.

The number of electrons collected is obtained from the mean ADU counts normalized to 1 second multiplied by the gain (electron/ADU). The optical power density is directly obtained from the IL1700 radiometer with a calibrated photodiode placed at the distance of the CCD plane and flux measurements are obtained in the range of 400 - 1000 nm in steps of 25 nm. The Qe is calculated using the above formula at different wavelengths

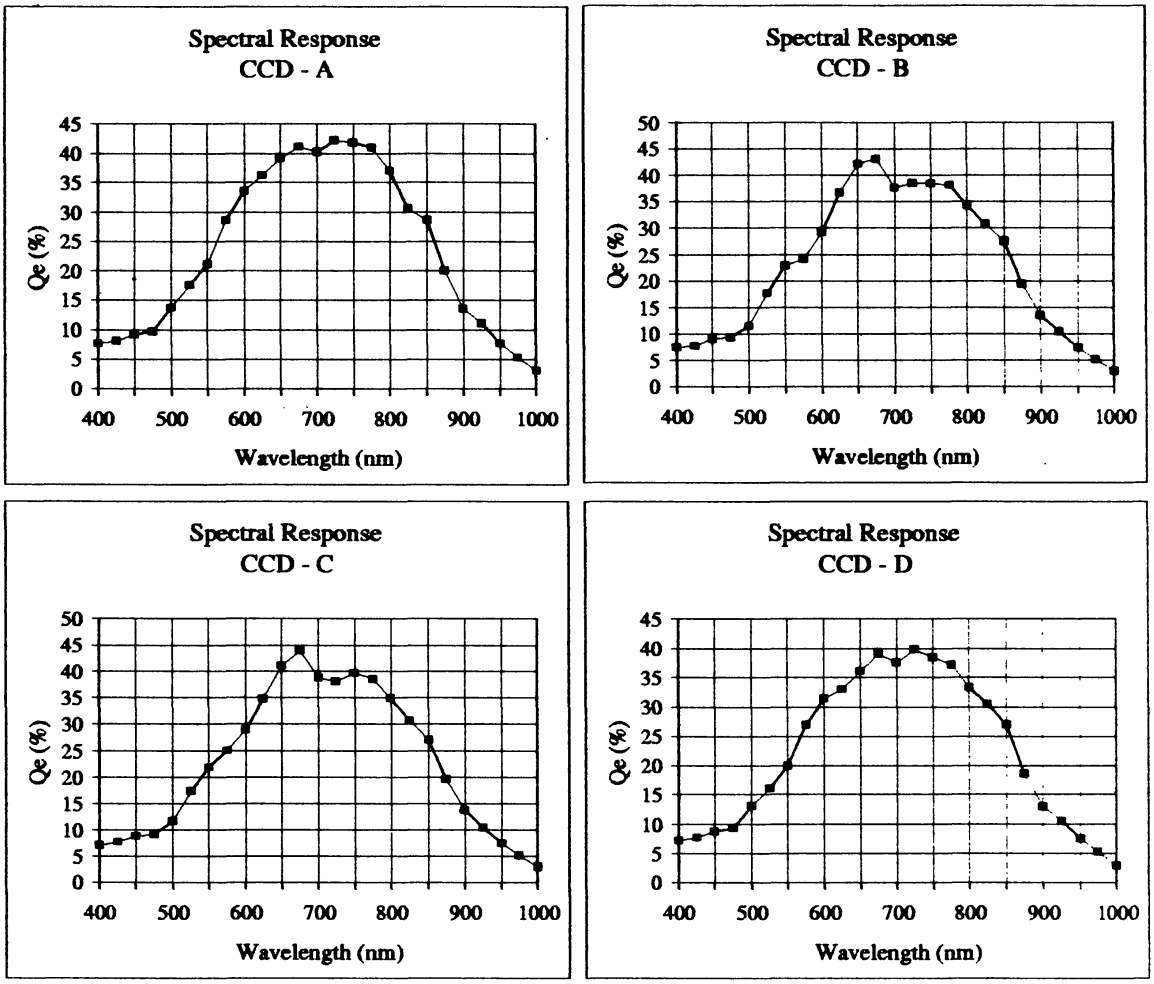

Figure 4. The spectral response of individual CCDs in the IIA mosaic camera.

and the spectral response is presented in Fig. 4 for all the 4 CCDs. Their peak Qe is in the red region with a value of $\sim$ 40 %. The value of Qe is more than 5 % over the entire range of measurements.

Fig. 5 shows the frequency distribution of the Qe at 800 nm for all the 4 mosaic CCDs. The mean Qe is about 35 % with $<$ 2 % rms non-uniformity. The percentages of pixels having Qe values more than 30 % are 99.7, 99.7, 98.9 and 97.7 for the CCD-A, B, C and D respectively.

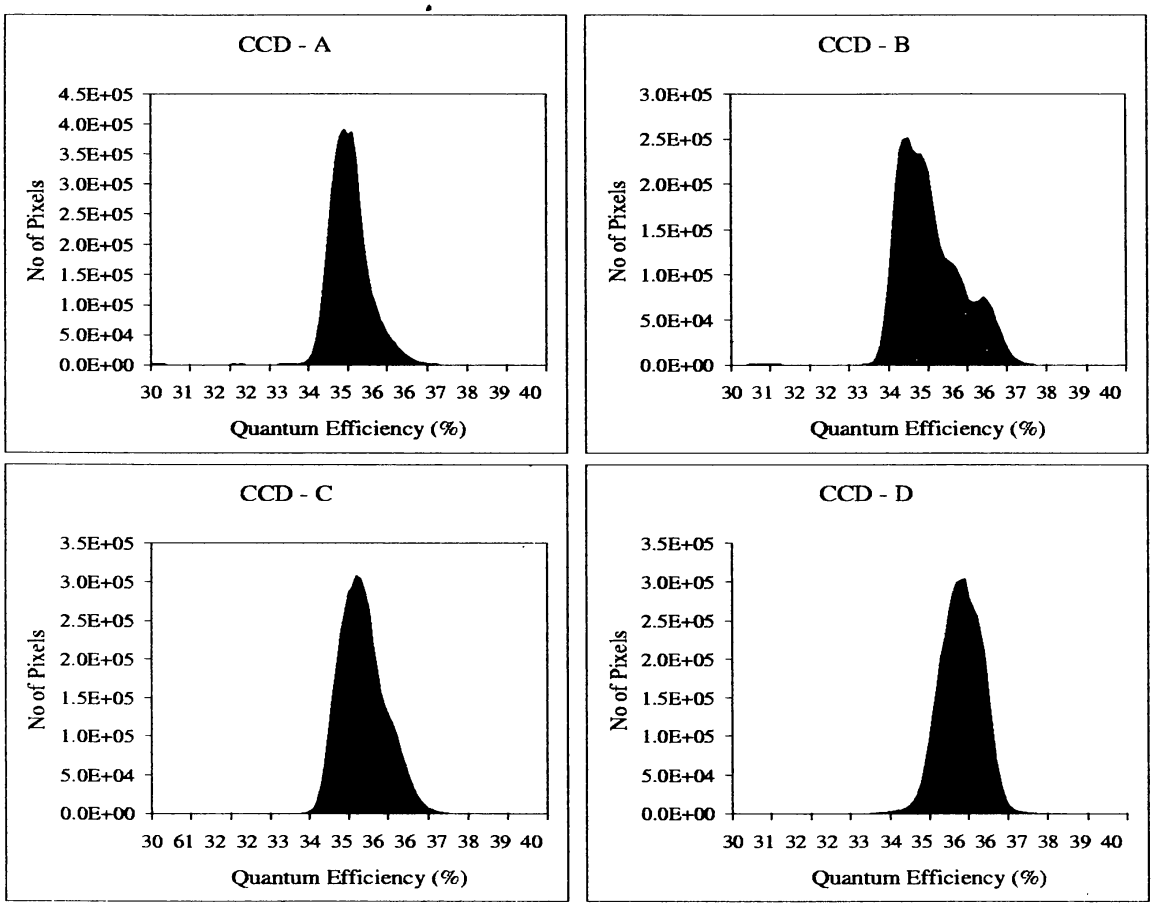

Figure 5. The histograms of Qe at 800 nm for individual CCDs of the IIA mosaic camera.

3.4 Linearity tests

The sets of data used to estimate the noise and gain are also used to plot the linearity curves. Fig. 6 shows a conventional linearity curve, mean count versus exposure time with a least-square linear equation fitted. The residuals of the fit provide an estimate of the non-linearities present in the system. To show the linearity residuals at less than 1 % level, a more useful plot is given in Fig. 7 which shows the measured mean count rate (signal counts/sec) corrected for the shutter delay against the exposure time. The shutter delay time is estimated by iteratively adjusting the exposure times and re-computing the ordinate data and fitting a straight line until best fit is found. The shutter delay time thus obtained is 72 ms. The CCDs are linear up to about 57 000 ADUs. The percentage of non-linearity (P-V) values are listed in both Fig. 7 and Table 1.

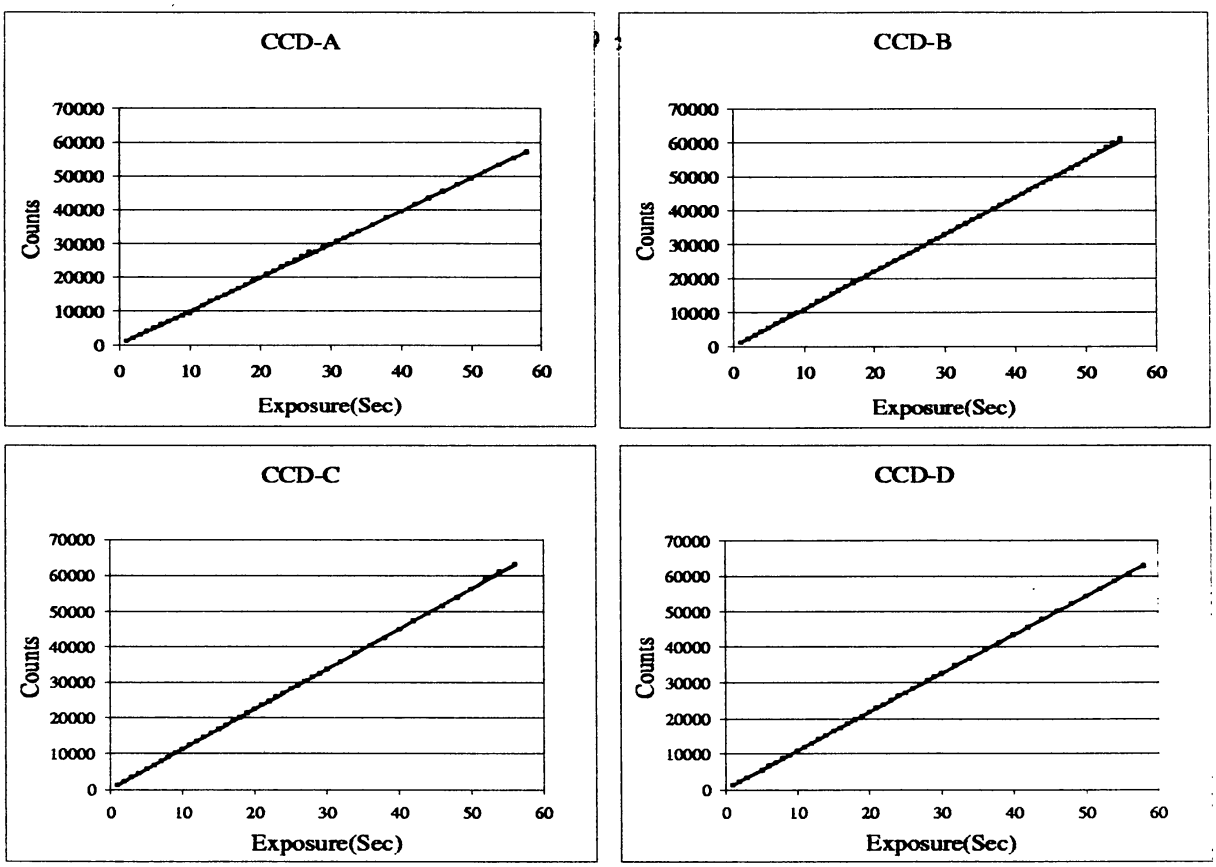

Figure 6. Linearity plots for individual CCDs of the IIA mosaic camera.

3.5 Traps and defects

Median stack frames obtained from a few low level flats ($\sim$ 2000 electron) are presented in Fig. 8 for all the 4 CCDs. The column defects (dark) and cluster of defects can be readily seen from these flats. The CCD-A has shown a large trap in the center of imaging area spanning over 1000 columns. The charge transfer subsequent to this trap is affected significantly till end. The CCD-B shows 7 column defects (7 columns x 1160 rows) towards the end (opposite to readout register) whose response is only 4 % compared with neighboring columns. The CCD-C is free from any significant defects. The CCD-D has also shown a cluster of column defects (22 columns x 660 rows) responding up to 17 %. This cluster defect is also towards the end and hence has no effects on further charge transfer.

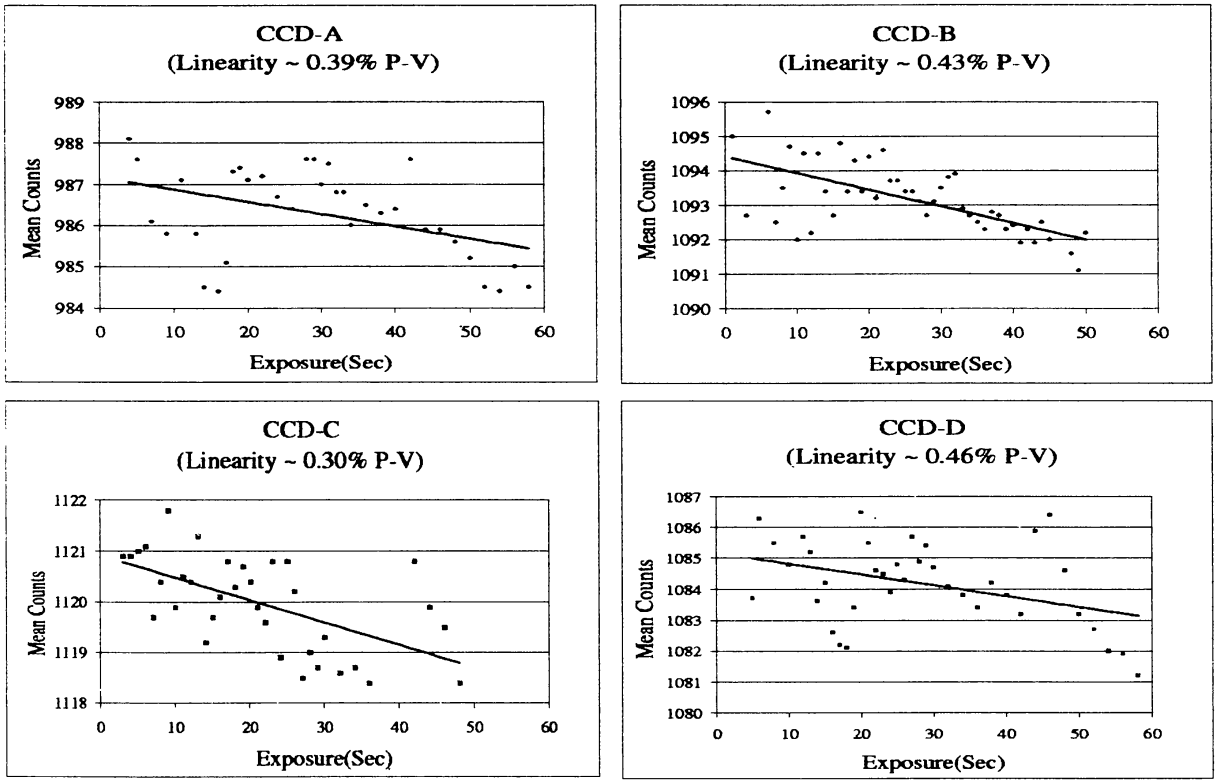

Figure 7. Linearity residual plots for CCDs in the IIA mosaic camera (mean counts are corrected for 0.072 sec shutter closing time).

3.6 Cross-talk in THX7897 devices

The reset FET and the output FET on the readout channel (Fig. 9) exhibit capacitance from their respective drain to source (CDS), controlling gate to channel etc. The CDS causes signal coupling from source to drain. The gate to channel capacitance causes the feed-through transients onto the signal when the FET is turned on or off. If the CCD has more than one-readout channel, the cross-channel capacitance inter-drain (CDD), inter-source (CSS) can also cause signal coupling between readout channels. The CDS capacitance of each FET on each channel couples some amount of signal onto their respective drains.

A section of an image acquired through one of the THX7897 device is shown in Fig.

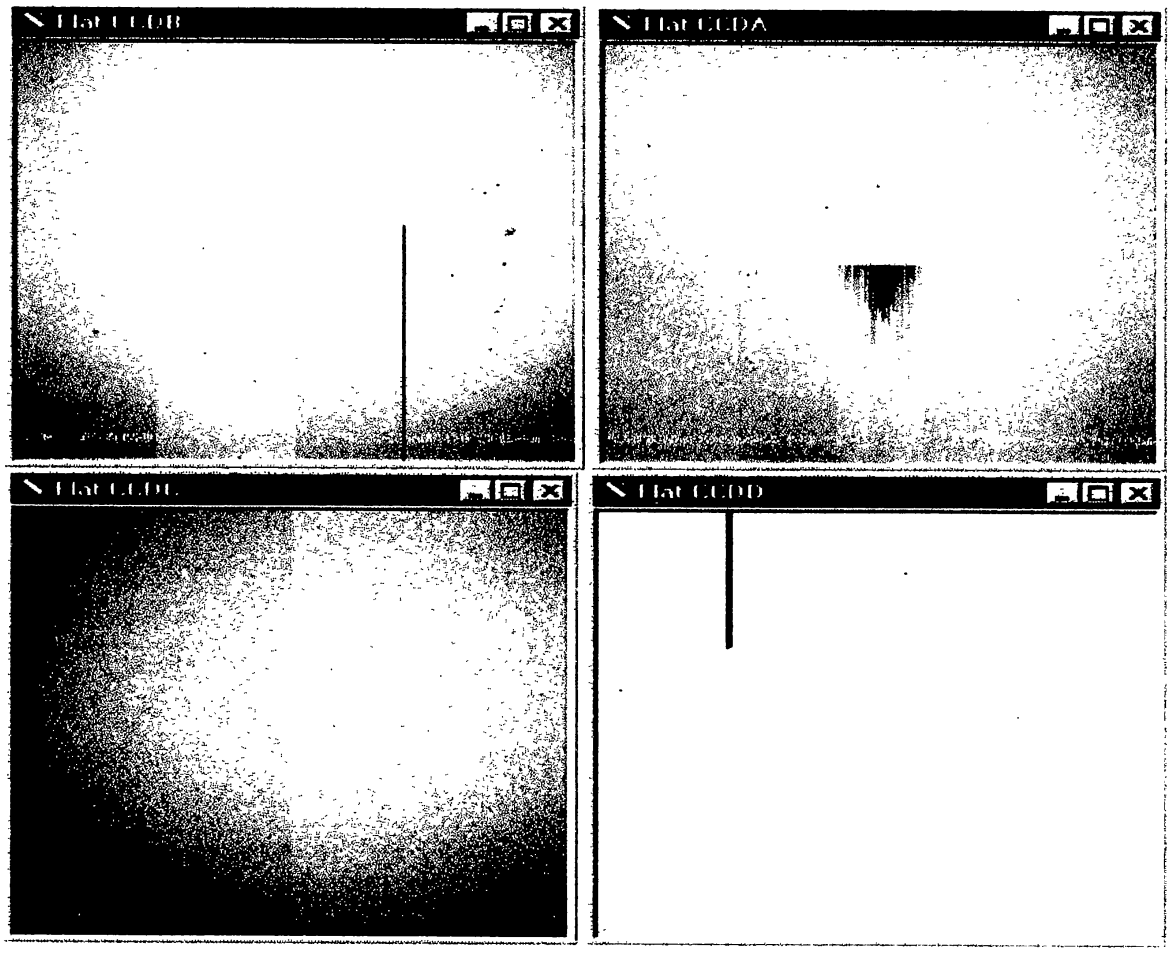

Figure 8. Low level flats showing the defects/traps.

10 where the signal coupling between readout channels can be seen. A signal coupling of about 3 - 4 % in the adjacent readout channels is noticed when all the Reset Drain (VDRi), Output Drain (VDDi) and MOS gate (VGMOSi) supplies (i = 1 to 4) of the readout channels are driven by their respective common voltage sources. If one of the readout channels sees a large signal, the other channels pickup a portion of this signal onto their readout values.

One way to eliminate this cross-talk is to provide independent buffers for the bias supplies (VDRi, VDDi and VGMOSi) of the readout channels. Suitable quad voltage buffers were introduced to provide independent bias voltages. This buffering completely eliminated the cross coupling due to the CDS capacitance. The cross coupling due to CDD or CSS is negligible, as they are physically distant from each other and not noticed in the THX7897 CCDs.

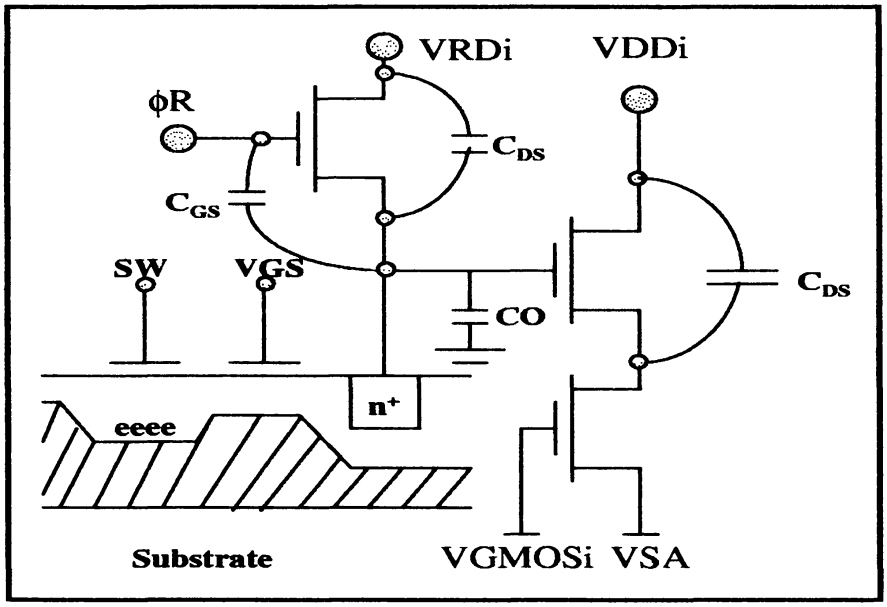

Figure 9. Readout stage-signal coupling path.

3.7 Bits distribution

A perfect ADC would generate equal number of 1s and 0s for white-noise input. For a well-exposed flat image, it is expected that the low order bits up to the illumination level should have almost equal number of 1s and 0s if there is no problems with the ADCs. Fig. 11 shows the distribution of 1s and 0s in a well-exposed flat field for the four CCDs in the mosaic. The solid line indicates fraction of bits which have 1s, while the dashed line is used for fraction of 0s. The 1s and 0s are almost equal for the lower order bits except for CCD-D, where a slight biasing towards more 0s is noticed.

4. Performance at the telescope

In order to evaluate the performance of the mosaic CCD at the telescope, it was mounted on the 104-cm Sampurnanand telescope of the State Observatory, Nainital (UPSO). Each pixel of this CCD corresponds to a square of 0.″24 size at the focal plane of the f/13 telescope beam. An open star cluster NGC 6631 was selected for observations. The choice of the cluster was made because the same cluster was earlier observed by Mohan, Lata & Sagar (2001) using the same telescope but UPSO 2K x 2K CCD system which

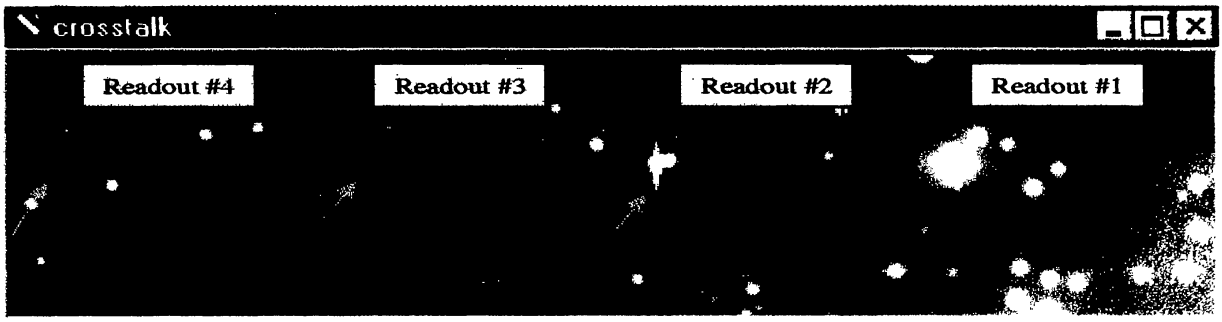

Figure 10. Cross-talk between readout channels.

Table 2. Transformation coefficients of the mosaic CCDs.

Coeff.	CCD-A	CCD-B	CCD-C	CCD-D
p1	1.078	1.081	1.087	1.077
p2	0.125	0.113	0.118	0.116

has a square pixel of 24 μm size and covers a square field of $\sim 13'$ size at the focal plane of the telescope.

The cluster was observed in V and I filters on May 9, 2001 using the mosaic CCD system. For calibration purpose, Landolt (1992) SA 107 and SA 110 standard fields were also observed along with a number of bias and twilight flat frames. The data reduction was carried out using IRAF and MIDAS software installed on the UPSO computers. The IRAF software package was used for cleaning, aligning and combining the images while the DAOPHOT software (Stetson 1987) was used for photometry. Images were bias subtracted and flat-fielded using standard reduction techniques. As the camera system is a mosaic of 4 CCDs, each CCD image was processed independently. The imaged cluster field is shown in Fig. 12 with individual CCD images marked as A, B, C and D. Further details of the observations and data reductions are given in the accompanying paper by Sagar, Naidu & Mohan (2001) along with the cluster parameters derived from the VI data of the stars in the NGC 6631 region.

The DAOPHOT software was used to perform aperture photometry for the standard stars. While observing, we placed a set of 7 standard stars on all the four CCDs of the mosaic. The calibration coefficients for all the 4 CCDs of the mosaic are determined using the following equations:

$$(V-I) = p1 \times (v-i)_0 + q1 \text{ and } V = v_0 + p2 \times (V-I) + q2,$$

where V and I are the standard values taken from Landoldt (1992) while v_0 and i_0 are the atmospheric extinction corrected instrumental CCD aperture magnitudes. The constants

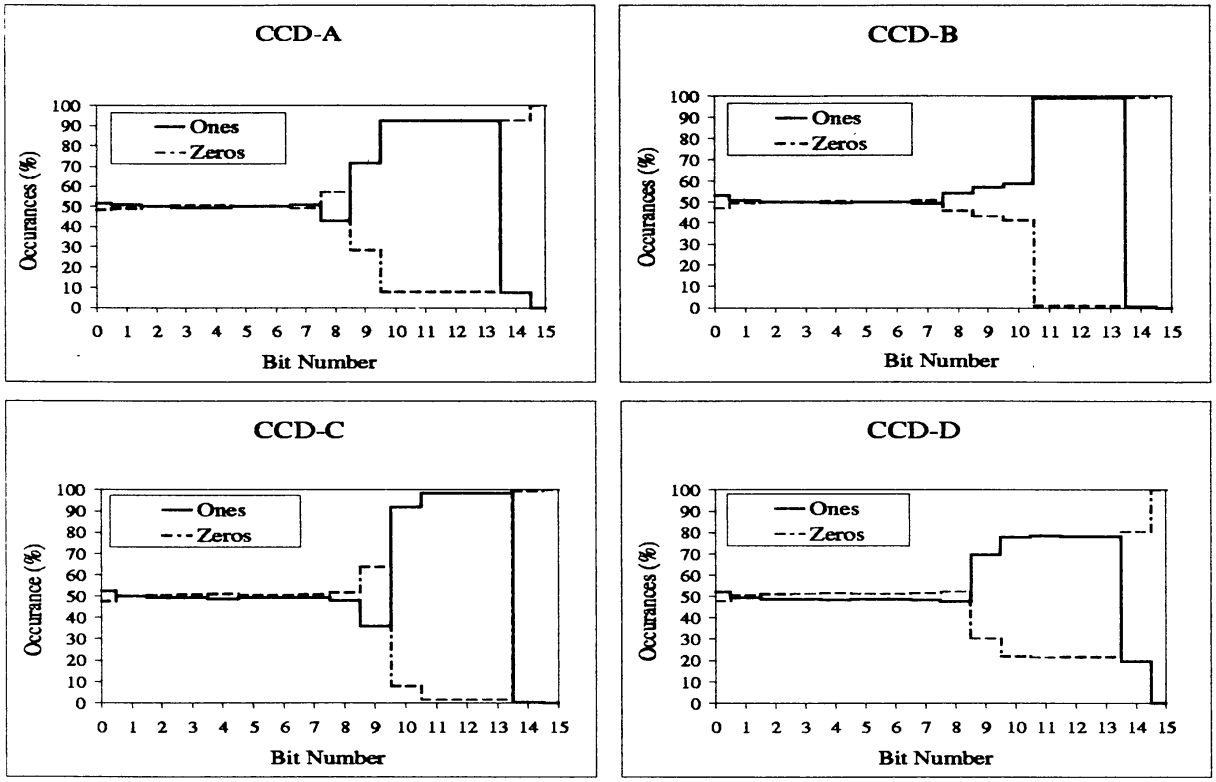

Figure 11. Histograms of bits of CCDs in the IIA mosaic camera.

p1 and p2 are the colour coefficients and q1 and q2 are the zero-points. The values of these constants for all 4 CCD chips are listed in Table 2. They indicate that the characteristics of all the 4 CCDs of the mosaic are almost identical and the filter combination closely reproduces the standard photometric system.

As there are physical gaps in the mosaic CCD system, it is necessary to precisely evaluate the dimensions of these gaps. This information is necessary to bring the positions of stars in different CCDs to a common reference. We have compared the position of stars in the cluster region observed through UPSO CCD with the positions observed in the present mosaic CCD system to evaluate these inter-gaps. Their values are shown in Fig. 12. Though the physical gaps are typically 0.8 mm, since each CCD has dead zones (no CCD pixels) of 0.2 mm on one side and 0.4 mm on other two sides, the physical gap between two CCDs is 1.2 mm in direction parallel to readout registers and 1.6 mm in its

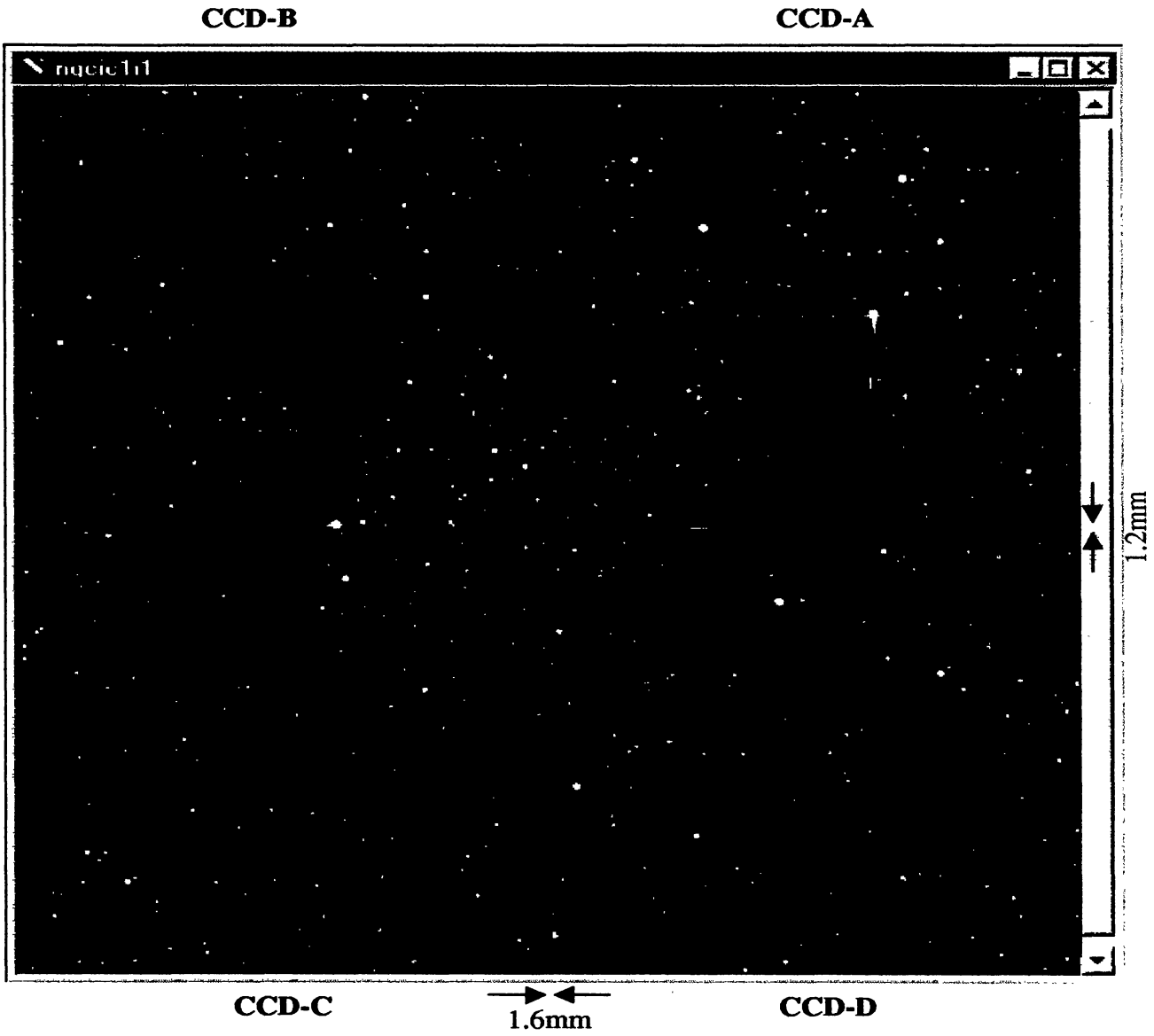

Figure 12. Imaged region of the open star cluster NGC 6631. Sizes of the physical gaps between the CCDs are marked.

perpendicular direction. We have also compared the magnitudes and colours obtained from the IIA mosaic CCD with those obtained from the UPSO CCD by Mohan et al. (2001). The differences in V and (V-I) magnitudes are plotted in Fig. 13 as a function of V magnitude and the statistical results are listed in Table 3. As expected, the scatter increases with decreasing brightness and becomes more than 0.1 mag for stars fainter than V = 18 mag. The estimated photon noise for stars of V = 17 and 18 mag are 0.003 and

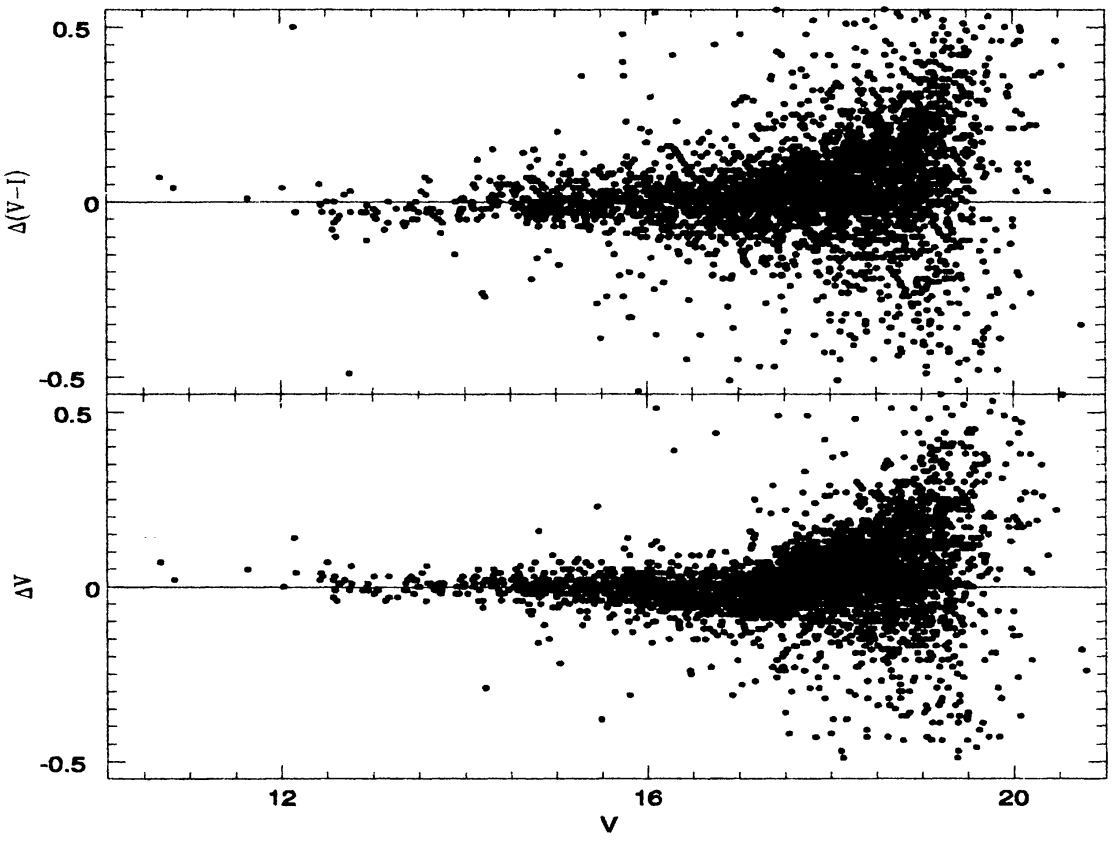

Figure 13. Comparison of the present CCD observations with those of the UPSO.

0.006 mag respectively. Considering these and the uncertainties present in photometric measurements, we conclude that the performance of the IIA 4K x 4K mosaic CCD system is satisfactory at an optical telescope.

5. Conclusions

The 4K x 4K mosaic CCD system developed at the IIA has been characterized. The laboratory experimental setup and characterization/calibration procedures are described. All the 4 CCDs in the mosaic show similar characteristics. The system gain and noise figures for the four CCDs are close to each other with values $\sim$ 3.9 electron/ADU and 19 electron respectively. The Qe curves are more or less same for all the 4 CCDs and closely agree with a typical THX7897 Qe curve. The cross-talk between the different readout sections could be eliminated by suitably buffering certain bias supplies. The

Table 3. Statistical results of the photometric comparison of the present VI CCD data with those obtained using the UPSO 2K x 2K CCD camera. The difference (Δ) is in the sense UPSO minus present data. The mean and standard deviation (σ) in mag are based on N stars. A few points discrepant by more than 3σ have been excluded from the analysis.

V Range	$\Delta V \pm \sigma$	N	$\Delta(V\text{-}I) \pm \sigma$	N
10-14	0.011±0.03	64	-0.021±0.04	63
14-16	0.001±0.03	361	-0.001±0.05	352
16-17	-0.021±0.04	420	-0.001±0.07	412
17-18	0.001±0.07	783	-0.021±0.09	784
18-19	0.041±0.10	1380	-0.061±0.14	1382
19-20	0.061±0.11	811	-0.081±0.15	813

performance of the mosaic CCD is evaluated by observing an open star cluster NGC 6631 and comparing the results obtained from previous observations of the same cluster by the UPSO 2K x 2K CCD system. The results indicate satisfactory performance of the IIA mosaic CCD camera system at the telescope.

Acknowledgements

The authors would like to thank the anonymous referee for useful comments. The realization of the mosaic CCD camera system has been possible due to efforts of many people in the electronics laboratory, mechanical workshop and the observational staff of the IIA. In particular, the authors would like to thank Mr. A.S. Babu, K. Ravi, S.V. Rao, A. Ramachandran for the electronics support. Mr. K. Sagay Nathan, V.K. Subramaniam extended their mechanical and CAD support. Thanks to the observational staff of the VBO, Kavalur and the UPSO, Nainital; and Mr. Brijesh Kumar (UPSO) for the coordination during observations.

References

Buil Christian, 1991, in CCD Astronomy, Willmann-Bell Inc Press, p. 51
Janesick J., Klaasen K. P., Elliott T., 1987, Opt. Eng., 26, 972
Landolt A. U., 1992, AJ, 104, 340
Mohan V., Lata S., Sagar R., 2001, (Private communication)
Naidu B. N., Srinivasan R., 2001, IEEE conference on Electro-Information Technology, Oakland University, Oakland, USA
Naidu B.N., Srinivasan R., Nathan K. S., 2001, BASI, 29, 135
Naidu B. N., Srinivasan R., Shankar S. M., 1997, Proc. of SPIE, 3114, 260
Sagar R., Naidu B. N., Mohan V., 2001, BASI, 29 (in press)
Stetson P.B., 1987, PASP, 99, 191